GEOPHYSICAL RESEARCH LETTERS, VOL. 33, L12604, doi:10.1029/2006GL026011, 2006

Global gridded data set of the oxygen isotopic composition in seawater

Allegra N. LeGrande[1] and Gavin A. Schmidt[1]

Received 9 February 2006; revised 4 April 2006; accepted 3 May 2006; published 21 June 2006.

[1] We present a new 3-dimensional 1° × 1° gridded data set for the annual mean seawater oxygen isotope ratio ($\delta^{18}O$) to use in oceanographic and paleoceanographic applications. It is constructed from a large set of observations made over the last 50 years combined with estimates from regional $\delta^{18}O$ to salinity relationships in areas of sparse data. We use ocean fronts and water mass tracer concentrations to help define distinct water masses over which consistent local relationships are valid. The resulting data set compares well to the GEOSECS data (where available); however, in certain regions, particularly where sea ice is present, significant seasonality may bias the results. As an example application of this data set, we use the resulting surface $\delta^{18}O$ as a boundary condition for isotope-enabled GISS ModelE to yield a more realistic comparison to the isotopic composition of precipitation data, thus quantifying the 'source effect' of $\delta^{18}O$ on the isotopic composition of precipitation. **Citation:** LeGrande, A. N., and G. A. Schmidt (2006), Global gridded data set of the oxygen isotopic composition in seawater, *Geophys. Res. Lett.*, *33*, L12604, doi:10.1029/2006GL026011.

1. Introduction

[2] The oxygen isotopic ratio of seawater ($\delta^{18}O$ – δ refers to the comparison of the sample isotopic ratio of $^{18}O/^{16}O$ to a standard) is a fundamental ocean tracer of both modern and past ocean circulation. Since $\delta^{18}O$ values in natural freshwater range widely, they can be used to determine the proportion of freshwater from multiple sources. The oxygen isotopic composition of precipitation is a tracer both of the modern hydrologic cycle (*International Atomic Energy Agency (IAEA)*, 2001), as well as past climate changes (e.g., in ice core and speleothem records). In the modern ocean, $\delta^{18}O$ has been used as a tracer for sea ice melt [e.g., *Macdonald et al.*, 1999], glacial and river runoff [e.g., *Khatiwala et al.*, 1999], deep ocean water masses [e.g., *Meredith et al.*, 1999], and deep water formation processes [e.g., *Jacobs et al.*, 1985].

[3] Paleoceanographic studies often use $\delta^{18}O$ as a proxy for climate since its variations through time are recorded by calcareous ocean organisms. The isotopic composition and the temperature of seawater during calcification determine the calcite isotopic composition, making calibrations between modern samples and oceanographic data (temperature and seawater $\delta^{18}O$) vital to the interpretation of this proxy record. World Ocean Atlas 2001 (hereinafter referred to as WOA01) [*Conkright et al.*, 2002] and others provide gridded data sets for the temperature portion of this calibration; however, no such gridded data set has existed for seawater $\delta^{18}O$.

[4] The sparseness of the observational data has inhibited the construction of a comprehensive global gridded data set of $\delta^{18}O$, and so seawater salinity has instead been used to estimate $\delta^{18}O$ [*Fairbanks et al.*, 1992]. The two are frequently linearly related since freshwater fluxes, including evaporation and precipitation closely affect both. However, the variation of $\delta^{18}O$ in the ocean is more complicated than salinity due to additional fractionation in the atmosphere [*Craig and Gordon*, 1965] and other processes, such as sea ice formation, that affect seawater $\delta^{18}O$ and salinity differently. These additional complications result in only regionally-coherent $\delta^{18}O$ to salinity ($\delta^{18}O$–S) relationships. In addition, $\delta^{18}O$ and, potentially, the $\delta^{18}O$–S relationship, vary on seasonal, annual, and inter-annual timescales.

[5] Recent improvements in data coverage combined with the need to have gridded data to compare to the distribution of water isotope tracers in global ocean and climate models have made the development of a gridded data set both possible and necessary. By clarifying our understanding of the variability of these isotopes, we hope to improve our understanding of the hydrologic cycle in general.

2. Methods

[6] Our basic data set for $\delta^{18}O$ comes from the *Schmidt et al.* [1999] online database (denoted $\delta^{18}O_{obs}$) which contains more than 22,000 measurements of $\delta^{18}O$ and salinity collected over 50 years, greatly extending the GEOSECS coverage that is generally taken as the standard reference [*Ostlund et al.*, 1987]. We consider all the data available to be broadly representative of the long term mean since the data set is too sparse to capture consistently seasonal or longer variability except in localized regions.

[7] We exclude points that are not representative of open-ocean conditions (see the updated online database) and omit estimated or incomplete data, including when the latitude, longitude, or measurements were read off of a graph. Some individual measurements are corrected for obvious typographical errors (such as a sign error) while highly anomalous data are excluded. We apply conversions from previous measurement standards to the current VSMOW (Vienna Standard Mean Ocean Water) standard. Some individual data sets have values for deep ocean water masses that are consistently offset from the analogous GEOSECS values. In these cases, we apply a constant correction for the entire data set ranging from 0.14‰ to 1.0‰ and noted the 7 affected data sets online.

[8] We sort the data into 24 distinct regions (Table 1). The surface ocean is divided into regions that are determined by surface circulation patterns and further subdivided

[1]NASA Goddard Institute for Space Studies and Center for Climate Systems Research, Columbia University, New York, New York, USA.

0094-8276/06/2006GL026011$05.00

Table 1. Regional $\delta^{18}O-S$ Relationships Determined for This Study and Basic Statistics

Water Mass	Total Points	Slope	Intercept	σ_{slope}	σ_{icept}	r^2	GEOSECS RMS Error	GEOSECS Points
Arctic Ocean	1846	0.48	−16.82	0.007	0.234	0.690	–	0
Deep Arctic Ocean	4484	0.84	−29.16	0.005	0.162	0.878	0.061	34
Baltic Seas	120	0.28	−8.73	0.013	0.109	0.806	–	0
GIN Seas	684	0.60	−20.71	0.014	0.466	0.744	0.224	6
Baffin Bay	492	0.33	−11.82	0.14	0.461	0.528	–	0
Labrador Sea	647	0.94	−32.45	0.014	0.490	0.87	–	0
Hudson Bay	376	0.42	−16.05	0.024	0.768	0.462	–	0
North Atlantic	743	0.55	−18.98	0.005	0.156	0.951	0.193	23
Tropical Atlantic	285	0.15	−4.61	0.008	0.297	0.552	0.131	16
South Atlantic	61	0.51	−17.40	0.013	0.449	0.963	0.118	15
Mediterranean Sea	131	0.28	−9.24	0.016	0.624	0.695	–	0
Red Sea/Persian Gulf	36	0.31	−10.81	0.014	0.518	0.938	–	0
North Pacific	751	0.44	−15.13	0.007	0.229	0.834	0.168	16
Tropical Pacific	286	0.27	−8.88	0.006	0.201	0.880	0.078	25
South Pacific	19	0.45	−15.29	0.028	0.996	0.936	0.080	19
Indian Ocean	332	0.16	−5.31	0.004	0.135	0.848	0.101	7
Southern Ocean	503	0.24	−8.45	0.014	0.478	0.374	0.132	16
NADW	1175	0.51	−17.75	0.007	0.230	0.851	0.105	155
Mixed Deep Water	449	0.42	−14.38	0.019	0.659	0.517	0.116	174
AABW	950	0.23	−8.11	0.019	0.661	0.131	0.075	44
Intermediate North Pacific	1106	0.43	−15.04	0.006	0.216	0.804	0.081	25
Deep Mediterranean Sea	377	0.41	−14.29	0.030	1.156	0.334	–	0
Deep Pacific/Indian	166	−0.41	14.25	0.179	6.206	0.031	0.078	60
CDW	1137	0.31	−10.85	0.013	0.439	0.346	0.075	93

into regions likely to have a distinct $\delta^{18}O$ signature; for example, the Greenland/Iceland/Norwegian (GIN) Seas is separate from the broader North Atlantic. Vertically, these surface regions extend to the deeper of 50 meters water depth or *Levitus and Boyer* [1994] monthly mixed layer depth (Z_m). We organize the data points into regions instead of taking the 'closest points' approach in order to minimize noise associated with extrapolations from much sparser data at the local level.

[9] Below the surface, regions are defined using water mass characteristics. In the Atlantic, we calculate PO_4* (corrected phosphate) from the WOA01 [*Conkright et al.*, 2002] oxygen and phosphate climatology and use it as a water mass tracer since deep waters from northern and southern sources have significantly different concentrations [*Broecker et al.*, 1998]. We define the North Atlantic Deep Water (NADW) end member as $PO_4^* < 1.1$ μmol/kg, the Antarctic Bottom Water (AABW) end member as $PO_4^* > 1.7$ μmol/kg, and assign water between these two end members to a combined region. Water in the Southern Ocean below Z_m and above 3000 meters is assigned to its own region (Circumpolar Deep Water). Southern Ocean water deeper than 3000 meters is assigned to the AABW region. In the subsurface North Pacific, intermediate water masses above 2500 meters are locally formed and assigned to their own region. Other intermediate waters in the Indian and Pacific Ocean are also defined separately (NADW/AABW mixture). Water depths below 2500 meters in these basins are assigned to a separate region.

[10] This distribution of regions is somewhat arbitrary but is driven both by the data coverage and basic descriptive oceanography and is designed to isolate areas where distinct $\delta^{18}O$-S relationships hold. We assign the available data into each region (taking into account monthly Z_m variations) and calculate a local linear least squares $\delta^{18}O-S$ relationship (Table 1). Some data points between 50 and 1000 meters could not be used due to a lack of information about when the sample was taken (and therefore whether or not it was above Z_m).

[11] Using the WOA01 1° × 1° grid, we make an initial estimate (denoted $\delta^{18}O_0$) based on the climatological salinity and the regional $\delta^{18}O-S$ relationship. The regions for the climatology are based on the annual mean Z_m, with a cap on maximum Z_m in the Southern Ocean at 100 meters, and smoothed over 5° × 5°. This procedure was found necessary to deal with inhomogeneities in the ocean climatology.

[12] To reduce unrealistic sharp transitions between regions, we use a 3-dimensional smoothing of $\delta^{18}O_0$ at each grid point with data from neighboring boxes (up to 550 km away) at each level and vertically up to three Z_m above and below the grid point. The data are weighed (equations (1a) and (1b)) to give preference to nearest neighbors; N.B., data from physically separate regions (such as the Atlantic and Pacific $\delta^{18}O$ values on either side of the Panama Strait) are not combined during this process. The product of this ellipsoid of $\delta^{18}O_0$ points provides a smoothed $\delta^{18}O$ value (denoted $\delta^{18}O_1$) at each grid box (equation (1c)).

$$H_{ij}(d_{ij}) = \exp\left[-\left(\frac{d_{ij}}{L}\right)^4\right] \qquad L \approx 550 \text{ km} \tag{1a}$$

$$H_z(d_z) = \exp\left[-\left(3\left(\frac{d_z}{Z_m}\right)\right)^4\right] \tag{1b}$$

$$\delta^{18}O_1 = \sum_{j}^{550\,km}\sum_{i}^{550\,km}\sum_{z}^{2*mld} H_{ij}(d_{ij})*H_z(d_z)*\delta^{18}O_0^{ijk} \tag{1c}$$

$$\delta^{18}O_2 = \frac{0.9\sum_n\left[\left(\delta^{18}O_{obs}\right)_n H(d_i)\right] + 0.1\delta^{18}O_1}{0.9\sum_n H\left(d_{ijz}\right)_{obs}^n + 0.1\sum_m H\left(d_{ijz}\right)_1^m} \tag{2}$$

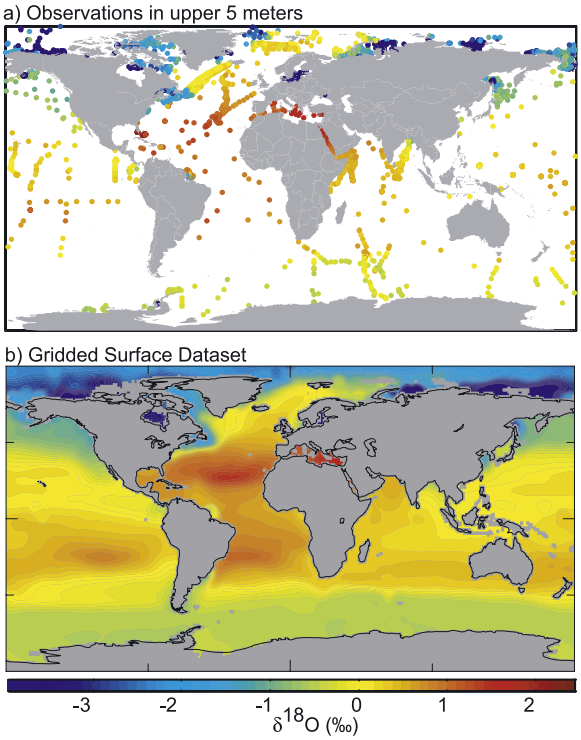

Figure 1. (a) All $\delta^{18}O$ measurements from the upper 5 meters of the water column [*Schmidt et al.*, 1999] illustrates good data coverage in the Arctic and Atlantic Oceans, but very sparse data in areas such as the Pacific and Southern Oceans; (b) the $1° \times 1°$ gridded data set of surface $\delta^{18}O$ calculated for this study agrees well in areas where there is good data coverage, and fills in areas with sparse or no data coverage based on both calculated $\delta^{18}O-S$ relationships and WOA01 salinity.

[13] The final estimate, $\delta^{18}O_2$, combines $\delta^{18}O_1$ with nearby $\delta^{18}O_{obs}$ values within each horizontal layer in the grid using the same distance weighting function (equation (1a)). We heavily weight (90%) $\delta^{18}O_2$ to the raw data where available (equation (2)). This final estimate provides a gridded data set of $\delta^{18}O$ that maximizes the use of all known $\delta^{18}O_{obs}$ values and fills in values at locations that have few or no known $\delta^{18}O$ values.

3. Results

3.1. Regional Relationships

[14] Data coverage varies greatly from region to region; therefore, the confidence for the regional relationships also varies. We include the correlation coefficients as well as the root mean-squared (RMS) error between the linear regression predicted $\delta^{18}O$ and GEOSECS data in each region (Table 1). Correlations are usually good, except in the deep oceans (the Southern Ocean, particularly), but often this is related to a narrow range of salinities, and so does not have a large effect on the final results. Some of the offsets from GEOSECS values are possibly related to seasonal or inter-annual variability, or to uncorrected data quality issues.

[15] The $\delta^{18}O-S$ slope is greatest at mid-latitudes and high northern latitudes and shallowest at low latitudes and the southern ocean [*Fairbanks et al.*, 1992; *Schmidt*, 1999]. At mid-latitudes, the freshwater end member is typical of local precipitation and the slope is quite high (~0.5‰/psu). In the tropics, the majority of water exchanged between the ocean and atmosphere remains in the region, implying a freshwater end member close to the initial evaporate and making the tropical slopes shallower (0.1 to 0.3‰/psu) than those in mid-latitudes.

[16] Sea ice (weakly) preferentially incorporates ^{18}O [*Craig and Gordon*, 1965; *Pfirman et al.*, 2004] and excludes salt, giving an opposite effect on the $\delta^{18}O-S$ relationship than observed in most other processes. In areas with sea ice formation and melting, $\delta^{18}O-S$ slopes tend to be shallow [*Tan and Strain*, 1996]. In the surface ocean, the influence of sea ice formation and melting yields water with a large range of salinities (several psu) without a large range of $\delta^{18}O$. Other areas with sea ice formation such as the Arctic Ocean have slightly higher correlations because of the larger range of salinities and $\delta^{18}O$, but a similar amount of scatter for salinities above 32 psu. Additionally, areas with seasonal sea ice changes may also have seasonal changes in the $\delta^{18}O-S$ relationship that we have not evaluated. Since these relationships combine data from all seasons from several decades, they should only be applied on shorter time periods with caution.

[17] The deep ocean does not maintain large salinity or $\delta^{18}O$ gradients, so even relatively sparse data coverage provides a reasonable estimate for average $\delta^{18}O$, including deep water masses whose sources are influenced by sea ice (such as the deep Southern Ocean).

3.2. Gridded Data Set

[18] The gridded data set agrees well with $\delta^{18}O_{obs}$ where there is data (Figures 1a and 1b). Database values across boundaries between different regions where there is sparse data coverage cannot be well quantified, and highlight the need for more $\delta^{18}O$ measurements. In particular, the frontal

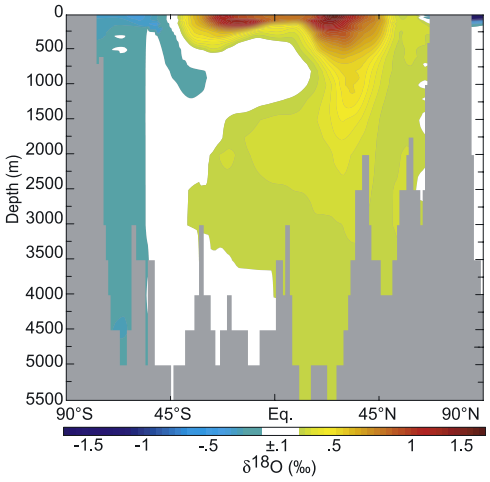

Figure 2. Vertical, 33-layer transect of the gridded $\delta^{18}O$ data set through the Atlantic Ocean 32.5°W (n.b., the pattern here is similar that of PO_4*, and illustrates the boundary between northern and southern end members). The $\delta^{18}O$ gradient across the Southern polar front (if any) is not well represented in the database, and we have left the visible boundary to indicate an area needing improvement.

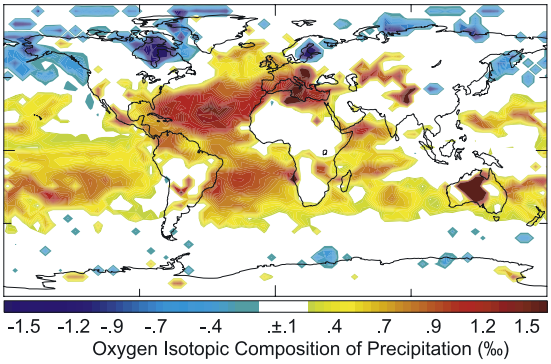

Figure 3. The simulated difference in the oxygen isotopic composition of precipitation using GISS ModelE between setting the surface boundary condition of $\delta^{18}O$ as in (Figure 1b) and defining it as 0‰ – The difference between the last 5 years of 11 year runs is plotted – values less than the students t-test 95% confidence are masked out.

region around the Southern Ocean is not well characterized. Other boundaries, such as across the Gulf Stream beyond Cape Hatteras, have sufficient data coverage to imply that the sharp $\delta^{18}O$ gradients seen in the gridded data are real.

[19] Vertically, the boundary between surface waters, intermediate, and deeper waters needs improvement. In the Atlantic, the large range of PO_4* concentrations provides an estimate for the boundary between the different water masses (Figure 2). In the other ocean basins, the data are not sufficient to define properly the range within intermediate waters, and the gridded data set would be improved by further seawater sampling at these intermediate depths. Our manipulation of the data has not significantly altered $\delta^{18}O$ compared to GEOSECS data (Table 1), and thus may be used in lieu of the GEOSECS data set with reasonable confidence.

3.3. Applications

[20] We anticipate that this gridded data set will provide a useful tool in paleoceanography and oceanography. It can provide additional information for water cycle modeling, as well as a comparison data set for isotope-enabled atmospheric and ocean models [*Schmidt*, 1999]. Paleoceanographic calibration studies can use this data set as a compliment to the *Levitus and Boyer* [1994] data set to calibrate coral, ostracod, and foraminiferal data sets [e.g., *LeGrande et al.*, 2004; *Schmidt and Mulitza*, 2002]. Water isotopes and their gradients may prove to be an additional constraint on surface water fluxes (evaporation, precipitation, river input), if good estimates (possibly from models) for the isotopic content of precipitation and evaporation can be obtained.

3.4. Example: Quantifying the Source Effect on the Isotopic Composition of Precipitation

[21] The oxygen isotopic composition depends on rainfall amount, surface air temperature, and initial water vapor isotopic composition. The relationship to rainfall and surface air temperature can be diagnosed from contemporaneous station data, but evaluating the influence of the initial source isotopic composition is more complicated.

[22] As an initial application of the gridded $\delta^{18}O$ data, we assess the impact of the initial source oxygen isotopic composition using GISS ModelE, an isotope-enabled atmospheric general circulation model [*Schmidt et al.*, 2006]. We use the gridded data set surface $\delta^{18}O$ as the surface ocean boundary condition and simulate the isotopic composition of precipitation for 11 years, and compare this result with an 11-year 'control' run that has surface ocean $\delta^{18}O$ defined as 0‰.

[23] The simulated effect of relatively more enriched surface waters in the Atlantic Ocean is isotopically heavier rainfall over the Atlantic basin and surrounding land masses (Figure 3). Water evaporated from the Mediterranean, in particular, is greatly enriched and yields a rain shadow of higher $\delta^{18}O$ across Europe and into Asia. The Arctic Ocean, North Sea, and Hudson Bay have significant input of river run-off, yielding relatively depleted surface $\delta^{18}O$ and thus lighter precipitation $\delta^{18}O$. The imposed changes to surface $\delta^{18}O$ improve the model simulation of isotopes in precipitation, reducing the bias from 0.6 to 0.3‰, slightly decrease the RMS error, and improve the spatial correlation when compared to observations [IAEA, 2001; *Schmidt et al.*, 2005].

4. Conclusions

[24] This first attempt at creating a global gridded data set should be treated as an experimental product. Better techniques, based on more tracer cross-correlations, for instance, might provide a more realistic $\delta^{18}O$ distribution. This study took a purely numerical approach, blending known values outward over a set distance. Future lines of investigation could include data assimilation into ocean circulation models to attempt to improve the representation of gradients and seasonal effects. This technique would likely better preserve sharp gradients of $\delta^{18}O$ in the ocean, and conceivably allow for better seasonal modulation.

[25] **Acknowledgments.** We would like to thank all of the contributors to the Global ^{18}O Seawater database for all of their individual efforts. ANL was funded by NDSEG Fellowship. GAS acknowledges the support of NSF grant OCE-99-05038 for work on ocean isotopes. We would like to thank NASA Giss for their institutional support.

References

Broecker, W. S., et al. (1998), How much deep water is formed in the Southern Ocean?, *J. Geophys. Res.*, *103*(C8), 15,833–15,844.

Conkright, M. E., R. A. Locarnini, H. E. Garcia, T. D. O'Brien, T. P. Boyer, C. Stephens, and J. I. Antonov (2002), World ocean atlas 2001: Objective analyses, data statistics, and figures CD-ROM documentation, *Internal Rep. 17*, pp. 1–21, Natl. Oceanogr. Data Cent., Silver Spring, Md.

Craig, H., and L. I. Gordon (1965), Deuterium and oxygen 18 variations in the ocean and the marine atmosphere, in *Stable Isotopes in Oceanographic Studies and Paleotemperatures*, edited by E. Tongiorgi, pp. 9–130, Cons. Naz. di Rech., Spoleto, Italy.

Fairbanks, R. G., C. D. Charles, and J. D. Wright (1992), Origin of global meltwater pulses, in *Radiocarbon After Four Decades: An Interdisciplinary Perspective*, edited by R. E. Taylor, A. Long, and R. S. Kra, pp. 473–500, Springer, New York.

International Atomic Energy Agency (IAEA) (2001), GNIP Maps and Animations, http://isohis.iaea.org/, Vienna, Austria.

Jacobs, S. S., R. G. Fairbanks, and Y. Horibe (1985), Origin and evolution of water masses near the Antarctic continental margin: Evidence from H218O/H216O ratios in seawater, in *Oceanology of the Antarctic Continental Shelf, Antarctic Research Series*, edited by S. S. Jacobs, pp. 59–85, AGU, Washington, D. C.

Khatiwala, S. P., R. G. Fairbanks, and R. W. Houghton (1999), Freshwater sources to the coastal ocean off northeastern North America: Evidence from $H_2{}^{18}O/H_2{}^{16}O$, *J. Geophys. Res.*, *104*(C8), 18,241–18,256.

LeGrande, A. N., J. Lynch-Stieglitz, and E. C. Farmer (2004), Oxygen isotopic composition of Globorotalia truncatulinoides as a proxy for intermediate depth density, *Paleoceanography*, *19*(4), PA4025, doi:10.1029/2004PA001045.

Levitus, S., and T. P. Boyer (1994), *World Ocean Atlas 1994*, vol. 4, *Temperature*, *NOAA Atlas NESDIS*, vol. 4, 129 pp., NOAA, Silver Spring, Md.

Macdonald, R. W., E. C. Carmack, F. A. McLaughlin, K. K. Falkner, and J. H. Swift (1999), Connections among ice, runoff and atmospheric forcing in the Beaufort Gyre, *Geophys. Res. Lett.*, *26*(15), 2223–2226.

Meredith, M. P., K. J. Heywood, R. D. Frew, and P. F. Dennis (1999), Formation and circulation of the water masses between the southern Indian Ocean and Antarctica: Results from delta O-18, *J. Mar. Res.*, *57*(3), 449–470.

Ostlund, H. G., H. Craig, W. S. Broecker, and D. Spenser (1987), GEOSECS Atlantic, Pacific, and Indian Ocean expeditions, in *Shore-based Data and Graphics*, vol. 7, pp. 1–200, Natl. Sci. Found., Washington, D. C.

Pfirman, S., W. Haxby, H. Eicken, M. Jeffries, and D. Bauch (2004), Drifting Arctic sea ice archives changes in ocean surface conditions, *Geophys. Res. Lett.*, *31*, L19401, doi:10.1029/2004GL020666.

Schmidt, G. A. (1999), Error analysis of paleosalinity calculations, *Paleoceanography*, *14*(3), 422–429.

Schmidt, G. A., and S. Mulitza (2002), Global calibration of ecological models for planktic foraminifera from coretop carbonate oxygen-18, *Mar. Micropaleontol.*, *44*(3–4), 125–140.

Schmidt, G. A., G. R. Bigg, and E. J. Rohling (1999), Global Seawater Oxygen-18 Database, http://data.giss.nasa.gov/o18data/, NASA Goddard Inst. of Space Sci., New York, N. Y.

Schmidt, G. A., G. Hoffmann, D. T. Shindell, and Y. Hu (2005), Modeling atmospheric stable water isotopes and the potential for constraining cloud processes and stratosphere-troposphere water exchange, *J. Geophys. Res.*, *110*, D21314, doi:10.1029/2005JD005790.

Schmidt, G. A., et al. (2006), Present day atmospheric simulations using GISS ModelE: Comparison to in-situ, satellite, and reanalysis data, *J. Clim.*, *19*, 153–192.

Tan, F. C., and P. M. Strain (1996), Sea ice and oxygen isotopes in Foxe Basin, Hudson Bay, and Hudson Strait, Canada, *J. Geophys. Res.*, *101*(C9), 20,869–20,876.

A. N. LeGrande and G. A. Schmidt, NASA Goddard Institute for Space Studies and Center for Climate Systems Research, Columbia University, 2880 Broadway, New York, NY 10025, USA. (legrande@giss.nasa.gov)